European Journal of Medicinal Chemistry 44 (2009) 2552–2562

Contents lists available at ScienceDirect

European Journal of Medicinal Chemistry

journal homepage: http://www.elsevier.com/locate/ejmech

Original article

Synthesis of 2-styrylchromones as a novel class of antiproliferative agents targeting carcinoma cells

Arthur Y. Shaw [a,*], Chun-Yi Chang [a], Hao-Han Liau [a], Pei-Jung Lu [b], Hui-Ling Chen [b], Chia-Ning Yang [c], Hao-Yi Li [c]

[a] Department of Chemistry, Tamkang University, Tamsui 251, Taiwan
[b] Institute of Clinical Medicine, National Cheng Kung University, Tainan 701, Taiwan
[c] Institute of Biotechnology, National University of Kaohsiung, Tainan 700, Taiwan

ARTICLE INFO

Article history:
Received 2 July 2008
Received in revised form
20 January 2009
Accepted 27 January 2009
Available online 6 February 2009

Keywords:
2-Styrylchromone
Antiproliferation
Carcinoma cells

ABSTRACT

A series of 2-styrylchromone analogs were synthesized and examined for their antiproliferative effects on a panel of carcinoma cells. Among the tested agents, only **4m** exhibited a moderate activity with an IC_{50} value of 28.9 μM against PC-3 cells which indicates the selectivity of PC-3 cells in response to 2-styrylchromones. In addition, **4q** demonstrated the most antiproliferative effect with an IC_{50} value of 4.9 μM against HeLa cells. Flow cytometric analysis and DAPI staining revealed that HeLa cells exposed to **4q** as low as 5 μM induced cell death through sub-G1 arrest and DNA fragmentation. Furthermore, CoMFA analysis of tested 2-styrylchromones resulted in a q^2 of 0.459 to generate a 3D-QSAR model on BT483 cell line. Together, these results suggest a potential structural optimization and pharmacological study of 2-styrylchromones.

© 2009 Elsevier Masson SAS. All rights reserved.

1. Introduction

Naturally occurring chromones (1-benzopyran-4-ones) are widely distributed throughout the plant kingdom [1–5]. These compounds have attracted a great deal of attention due to their substantial activities, including antioxidative and anticancer effects [6–11]. Accordingly, many synthesized chromone derivatives have been extensively studied for the development of novel anticancer agents. Molecular mechanisms of anticancer effects mediated by chromones such as flavonoids could be attributed to antiproliferation, induction of apoptosis, cell cycle arrest, promotion of differentiation, inhibition of angiogenesis, and modulation of multidrug resistance [12]. Among these chromone derivatives, flavopiridol (**I**) has been identified as a cyclin-dependent kinase (CDK) inhibitor and it has entered in Phase II clinical trial [13,14]. 2-Styrylchromones are a small group of chromones with only two natural 2-styrylchromones hormothamnione (**II**) and 6-desmethoxyhormothamnione (**III**) are known (Fig. 1).

Hormothamnione was isolated in 1986 from the marine cryptophyte *Crysophaeum taylori* [15]. Its 6-desmethoxy analog was characterized in 1989 from the extracts of the same blue-green algae [16]. Hormothamnione demonstrated potent cytotoxicity against P388 lymphocytic leukemia and HL 60 human promyelotic leukemia cell lines, while 6-desmethoxyhormothamnione exhibited antitumor activity against 9 kb and colon 38 tumor cells, respectively. A number of synthesized 2-styrylchromone derivatives have shown to exhibit antiallergic [17], antiviral [18], antitumor [19], anticancer [20,21], and antioxidant activities [22,23], and to serve as antagonism of A3 adenosine receptor [24], and xanthine oxidase inhibitors [25]. Among all biological activities, the anticancer effect is of particular interest that we decided to synthesize and evaluate the antiproliferation of a series of 2-styrylchromones against a panel of carcinoma cell lines. Herein, we report the synthesis of 2-styrylchromones based on the modifications of ring-B and ring-A as shown in Fig. 1. Mechanistic study of antiproliferative effect mediated by the representative compound **4q** is examined in this paper. Moreover, 3D-QSAR model established by CoMFA analysis on BT483 cell line is studied as well.

2. Results and discussion

2.1. Chemistry

Various strategies have been developed for the synthesis of 2-styrylchromones, all including the formation of a carbon–carbon bond as the key step [26,27]. As shown in Scheme 1, our initial goal was to synthesize the 2-styrylchromone scaffold with

* Corresponding author. Tel.: +886 2 2621 5656x2842; fax: +886 2 2620 9924.
E-mail address: shaw299@mail.tku.edu.tw (A.Y. Shaw).

0223-5234/$ – see front matter © 2009 Elsevier Masson SAS. All rights reserved.
doi:10.1016/j.ejmech.2009.01.034

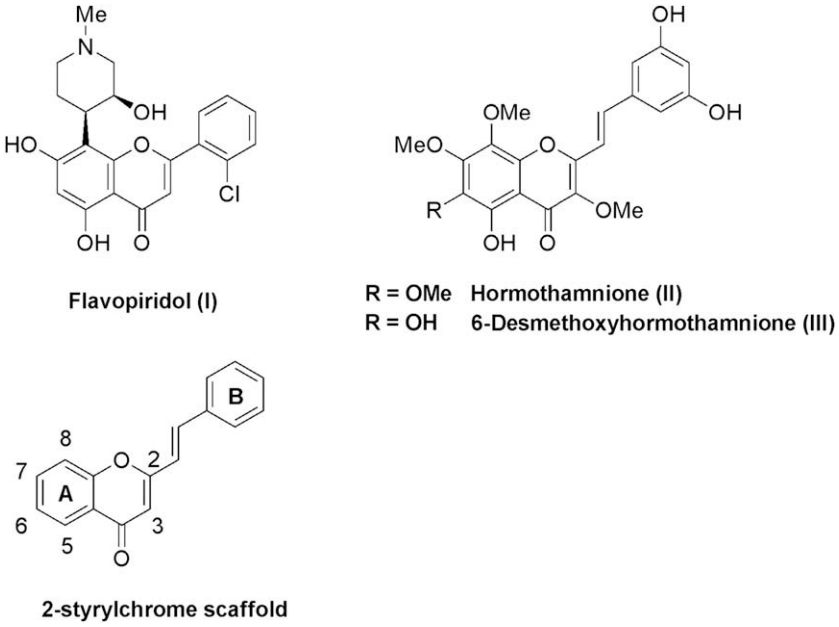

Fig. 1. Chemical structures of chromone derivatives.

5,7-dimethoxy 2-styrylchromones with different substituents in the ring-B moiety designated in Fig. 1.

To carry out the synthesis of 2-styrylchromone analogs **4a**–**4l**, commercially available 2′,4′,6′-trihydroxyacetophenone (**1a**) was subjected to dimethylation reaction reported by Gray et al. [28] with slight modification (Scheme 1). Treatment of **1a** with two equivalents of dimethylsulfate in the presence of potassium carbonate in acetone solution at room temperature for 18 h afforded 2′,4′-dimethoxy-6-hydroxyacetophenone (**2a**) in good yields. We attempted to synthesize 2-methyl-5,7-dimethoxychromone (**3a**) via a Claisen condensation of **2a** with ethyl acetate but obtained low conversion rates. Therefore, an alternative method was adopted in which **2a** was dissolved in the neat ethyl acetate solution with six equivalents of sodium at room temperature to give 1,3-diketone intermediate (monitored by TLC plate) [29]. Without further purification, 1,3-diketone intermediate was treated with couple drops of concentrated HCl in methanol to obtain 2-methyl-5,7-dimethoxychromone (**3a**) with good yield (67% in two steps). With the crucial chromone intermediate **3a** in hand, a series of 2-styrylchromone derivatives (Table 1) were successfully synthesized under similar conditions [30]. For example, **4a** was prepared by the condensation of **3a** with benzaldehyde in the presence of sodium methoxide and methanol at reflux for 18 h. It is noteworthy that benzaldehydes bearing electron-donating groups such as 4-methoxy (**4f**), 1,2-methylenedioxy (**4g**) retarded the condensation that an appreciable heat and extended reaction time were required to accomplish the reaction. In contrast, benzaldehydes with electron-withdrawing groups such as 4-fluoro (**4c**), 4-chloro (**4d**), 4-bromo (**4d**) 4-trifluoromethyl (**4i**), 4-trifluoromethoxy (**4j**) and 4-nitro (**4k**) are more reactive that condensation could be carried out at ambient temperature and reduced reaction time.

Modification of ring-A indicated in Fig. 1 was focused on the introduction of methoxy groups at different positions in the chromone scaffold. The preparation of all the analogs was carried out according to the synthetic route shown in Scheme 2.

Compounds **4m**–**4q** were synthesized according to their corresponding acetophenones **2m**–**2q**. In addition, we employed the 4-trifluoromethoxy (4-OCF_3) group in ring-B as a serial modification because preliminary antiproliferation screens indicated that **4j** exhibited the most potent activity against A431 skin carcinoma cancer cells with 95% growth inhibition at 25 μM treatment (data not shown). Therefore, as chromone intermediates **3m**–**3q** were prepared, the final condensation to obtain 2-styrylchromone analogs **4m**–**4q** were successfully achieved and ready for the antiproliferation study.

2.2. Antiproliferation study

In this study 2-styrylchromone derivatives **4a**–**4q** were screened in vitro against a panel of five human carcinoma cell lines, including PC-3 (prostate carcinoma cell), A549 (non-small cell lung

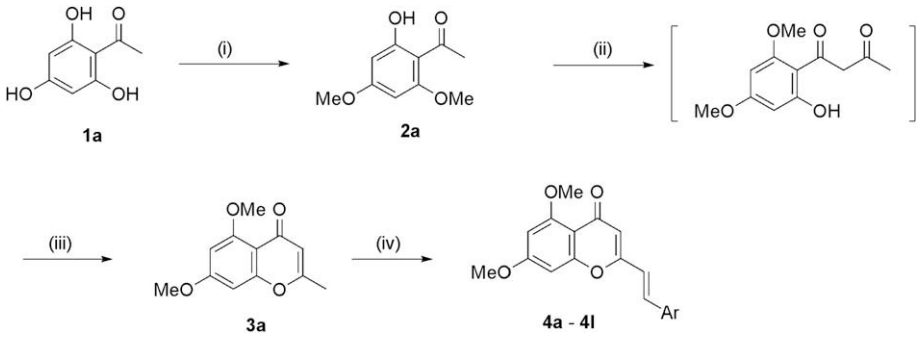

Scheme 1. Reagents and conditions: (i) Me_2SO_4/K_2CO_3, acetone; (ii) Na/EtOAc; (iii) conc. HCl/MeOH; (iv) MeONa/ArCHO/MeOH.

Table 1
Chemical structures of 2-styrylchromone derivatives **4a** to **4l**

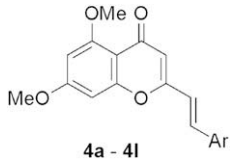

4a - 4l

Compound	Ar	Compound	Ar
4a	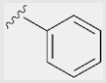	**4g**	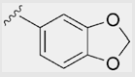
4b	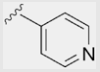	**4h**	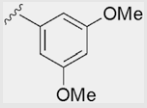
4c	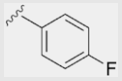	**4i**	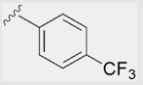
4d	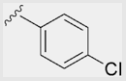	**4j**	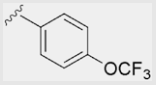
4e	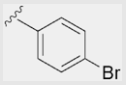	**4k**	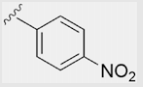
4f	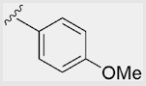	**4l**	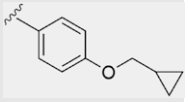

adenocarcinoma cell), BT483 (mammary gland adenocarcinoma cell), HeLa (cervical epithelioid carcinoma cell) and SKHep (hepatocellular carcinoma cell). The MTT (3-[4,5-dimethylthiazol-2-yl]-2,5-diphenyltetrazolium bromide) assay [31] was employed for these antiproliferation studies and the IC_{50} values are summarized in Table 2. The compound concentration causing a 50% cell growth inhibition (IC_{50}) was determined by interpolation from dose–response curves.

Surprisingly, among all tested agents, only **4m** (IC_{50}, 28.9 μM) exhibited moderate activity against PC-3 cells. For example, modifications of 2,5-dimethoxy 2-styrylchromone analogs in ring-B with different stereochemical properties (**4a**–**4l**) did not suppress the cell proliferation, indicating neither steric nor electronic effects of various substituents in the ring-B show significant effect on PC-3 cells. It is noteworthy that **4m** without any methoxy groups in the ring-A exhibited the most antiproliferative effect, suggesting either steric or electronic property of methoxy group could decrease the antiproliferative activity of 2-styrylchromones. Therefore, we concluded that selective antiproliferation of PC-3 cells to the tested compounds could be mainly attributed to both steric and electronic effects of ring-A rather than ring-B moiety in the 2-styrylchromone structure.

Exposure of A549 cells to the tested compounds also revealed certain degree of selectivity. For instance, compound **4a** and its 4-fluoro counterpart **4c** exhibited comparably moderate antiproliferative activity with IC_{50} values of 21.5 and 18.6 μM, respectively. However, replacement of phenyl group of **4a** to 4-pyridiyl group of **4b** resulted in the loss of the antiproliferative effect. This might be due to disfavored interactions between the hydrogen-bond acceptor of **4b** and its molecular targets that counteract the overall activity. Compared to **4c** bearing a 4-fluoro group in ring-B, analogs with bulkier substituents such as 4-chloro (**4d**), 4-bromo (**4e**), 4-methoxy (**4f**) and 4-trifluoromethyl (**4i**) did not show any antiproliferative effects on A549 cells. Interestingly, 4-substituted analogs with either electron-withdrawing groups such as 4-trifluoromethoxy (**4j**) and 4-nitro (**4k**) or an extended side chain like 4-cyclopropylmethoxy (**4l**) exhibited moderate activities with IC_{50} values of 24.2, 19.7 and 20.9 μM, respectively. Furthermore, **4h** bearing 3,5-dimethoxy group (IC_{50}, 15.6 μM) rather than **4g** (IC_{50}, >40 μM) with 3,4-dioxomethylene group exhibited relatively better activity against A549 cells. Together, these results indicated plausible correlations between structural characteristics of the tested compounds with their antiproliferative effects on the A549 cells. Similar to data indicated in the PC-3 cells, only **4m** (IC_{50}, 15.6 μM) demonstrated a moderate activity against A549 cells among modified ring-A 2-styrylchromone analogs.

Results of BT483 cells exposed to the tested compounds showed that most compounds exhibited moderate potency with IC_{50} values in a range of 15.5–30.9 μM. In contrast to the results shown in A549, HeLa and SKHep cells, **4a** exhibited no activity against BT483 cells. Additionally, **4e** bearing 4-bromo group of ring-B was not active against the tested carcinoma cells. On the other hand, 3,5-dimethoxy group of **4h** and an extended side chain of **4l** exhibited relatively higher activities against BT483 cells with IC_{50} values of 16.6 and 16.5 μM respectively, which were 1.7-fold more potent than their counterpart **4f** (IC_{50}, 29.6 μM), suggesting that certain space of ring-B is amenable to structural optimization. Among modified ring-A analogs, most of the tested compounds exhibited moderate activities except for **4o** with 6-methoxy group, this might be due to the repulsive interactions such as the steric hindrance between **4o** and its molecular targets. Instead, **4m** bearing no substituent showed the most potent antiproliferative activity with an IC_{50} value of 15.5 μM.

Interestingly, HeLa cells seemed to be the most sensitive to the tested compounds among five carcinoma cell lines. Most compounds displayed better antiproliferative effects on HeLa cells. Among them, compound **4q** exhibited the most potent antiproliferative activity with an IC_{50} value of 4.9 μM while **4j** with 4-trifluoromethoxy was not active among the ring-A modified analogs. Basically, no distinct antiproliferative structure–activity relationship was observed in this series of 2-styrylchromones against HeLa cells. SKHep cells were not as sensitive as HeLa cells toward the tested compounds in which **4j** and **4q** showed better antiproliferative activity with IC_{50} values of 12.5 and 12.4 μM respectively.

In an effort to further investigate the antiproliferative effects mediated by **4q** on the HeLa cells, total 30 h period of growth time was monitored. The growth curves showed that **4q** can suppress the cell proliferation in a dose-dependent manner. After 30 h of treatment shown in Fig. 2, **4q** exhibited about 60% and 15% of cell proliferation at 10 and 3 μM, respectively. Fig. 3 demonstrates the incubation of the HeLa cells with different concentrations of **4q** after 24 h treatment with significant morphological changes including cell rounding and detachment from the substratum.

Recently, synthetic 4-methoxy-2-styrylchromone has been reported to be a microtubule-stabilizing antimitotic agent that blocks G2/M phase of the cell cycle [20]. To examine the association

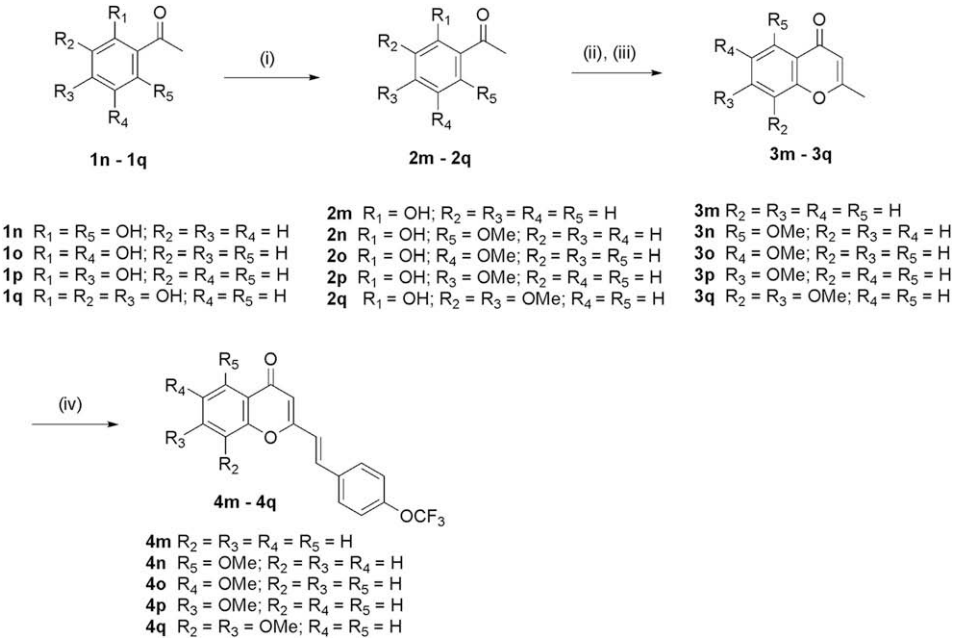

Scheme 2. Reagents and conditions: (i) Me_2SO_4/K_2CO_3, acetone; (ii) Na/EtOAc; (iii) HCl/MeOH; (iv) MeONa/4-$OCF_3C_6H_4CHO$/MeOH.

between 2-styrylchromone-induced antiproliferation and cell cycle arrest, we selected **4a**, **4i** and **4q** to analyze the cell cycle distribution by flow cytometry. Exposure of HeLa cells to 20 μM of **4a** and **4i** for 24 h was found to exhibit a certain amount of G1 phase cell cycle arrest as shown in Fig. 4E and F, respectively. Nevertheless, **4q**-induced sub-G1 phase arrest was observed in a dose-dependent manner as shown in Fig. 4C and D, indicating that antiproliferative effect on HeLa cells mediated by **4q** may be attributed to the DNA fragmentation and resulting in cell death.

To further demonstrate **4q**-mediated antiproliferation via the induction of DNA fragmentation, DAPI staining of HeLa cells at 5 μM and 10 μM of **4q** treatment was carried out. As shown in Fig. 5A, DNA fragmentation effect was clearly observed upon 10 μM of **4q** treatment. Moreover, to investigate whether **4q** exhibits microtubule-stabilizing effect as similar to that of reported in the literature [20], immunocytochemistry and in vitro tubulin polymerization assays were examined. As shown in Fig. 5B, treatment of **4q** at 10 μM did not interfere with microtubule assembly compared to untreated control (Mock). Moreover, tubulin polymerization assay (Fig. 5C) revealed that **4q** did not exhibit microtubule-stabilizing effect that is correspondent with the observations in flow cytometric analysis. In summary, these results suggest that some of our compounds could induce the antiproliferative effect on HeLa cells through distinct mechanisms such as G1 phase cell cycle arrest and DNA fragmentation.

Table 2
Cytotoxicity of 2-styrylchromones against carcinoma cell lines. IC_{50} are presented as the mean ± sem (standard error of the mean) from four to six separated experiments.

Compound	IC_{50}(μM)				
	PC-3	A549	BT483	HeLa	SKHep
4a	>40	21.5 ± 4.1	>40	10.1 ± 1.9	26.0 ± 0.9
4b	>40	>40	25.2 ± 1.7	18.8 ± 2.2	>40
4c	>40	18.6 ± 0.6	19.9 ± 2.2	14.2 ± 1.2	29.2 ± 0.8
4d	>40	>40	26.1 ± 2.2	14.2 ± 1.4	26.9 ± 7.1
4e	>40	>40	>40	>40	>40
4f	>40	>40	29.6 ± 1.4	17.8 ± 2.5	>40
4g	>40	>40	29.3 ± 2.9	16.4 ± 2.8	23.7 ± 7.6
4h	>40	15.6 ± 2.6	16.6 ± 2.4	16.7 ± 2.9	23.7 ± 3.0
4i	>40	>40	>40	19.0 ± 1.5	20.6 ± 4.0
4j	>40	24.2 ± 1.5	26.6 ± 3.0	>40	12.5 ± 2.9
4k	>40	19.7 ± 4.6	25.5 ± 1.9	9.6 ± 1.6	22.0 ± 1.3
4l	>40	20.9 ± 5.9	16.6 ± 1.3	10.9 ± 2.2	22.1 ± 0.4
4m	28.9 ± 0.7	15.6 ± 1.9	15.5 ± 1.9	15.9 ± 2.5	>40
4n	>40	>40	18.2 ± 2.3	9.1 ± 2.5	21.0 ± 0.4
4o	>40	>40	>40	9.0 ± 2.0	>40
4p	>40	>40	20.1 ± 2.2	9.9 ± 1.6	>40
4q	>40	>40	30.9 ± 1.1	4.9 ± 1.0	12.4 ± 1.5

2.3. 3D-QSAR on BT483 cell line

To gain insight into the structure–activity relationship between 2-styrylchromones and carcinoma cells tested in this study,

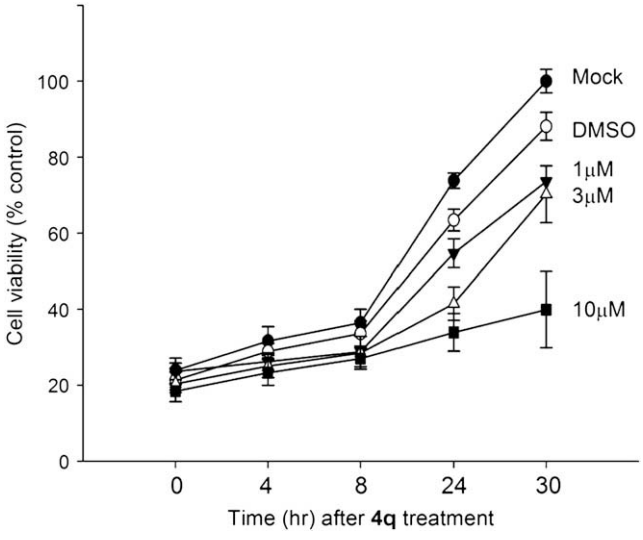

Fig. 2. Antiproliferative effect of **4q** on HeLa cells. Adherent cells proliferated in 96-well plates (10^4 cells/well) were incubated with different concentrations of **4q** (1.0, 3.0 and 10 μM) compared to untreated control (Mock) and 0.1% DMSO treatment, and determined by MTT assay at various time intervals.

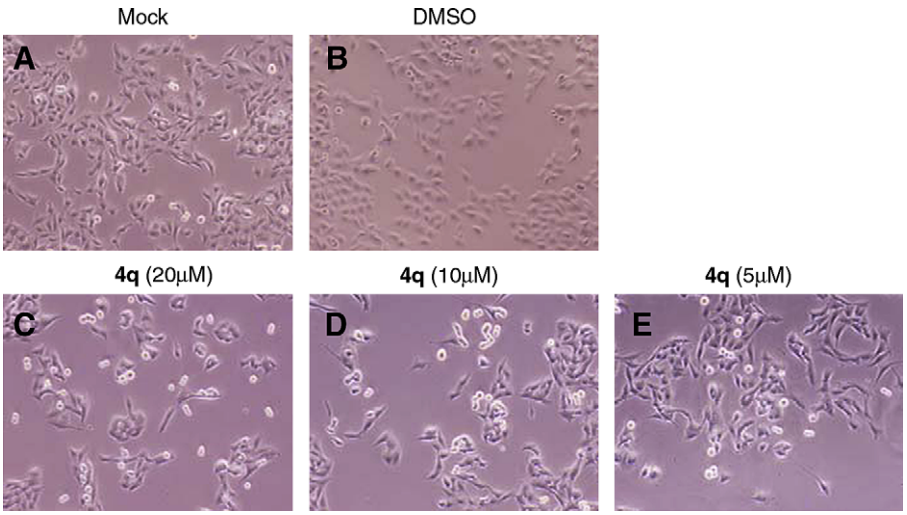

Fig. 3. Morphological analysis for the effects of **4q** on HeLa cells after 24 h incubation. (A) Untreated control. (B) DMSO treatment. (C) **4q** at 20 μM treatment. (D) **4q** at 10 μM treatment. (E) **4q** at 5 μM treatment.

comparative molecular field analysis (CoMFA) was performed by Sybyl 8.0 (Tripos International, 1699 South Hanley Road, St. Louis, Missouri 63144, USA) to investigate how substituents influence the activities of the BT483 cell line. We chose to investigate BT483 results rather than other cell lines due to its higher sensitivity and selectivity toward the studied compounds according to our empirical data. The studied 17 structures with charge assignment done with Gasteiger–Marsili method were generated for CoMFA analysis and by applying 100 steps in steepest descent algorithm followed by 500 steps in conjugate gradient algorithm for geometry minimization without constraints on the internal geometry of the molecules. The alignment of compounds plays a critical role in determining structure–activity relationship. For the binding site is unknown, we assumed that each compound would adopt a conformation in its lowest energy. Database alignment protocol in Sybyl 8.0 was utilized to pairwise align the structures according to the core conformational template specified in ball and stick as shown in Fig. 6A. To build CoMFA model, the CoMFA descriptors, steric (Lennard–Jones 6–12 potential) and electrostatic (Coulombic potential) field energies were calculated with an sp^3 carbon atom carrying +1.0 charge to serve as a probe atom using Sybyl default parameters.

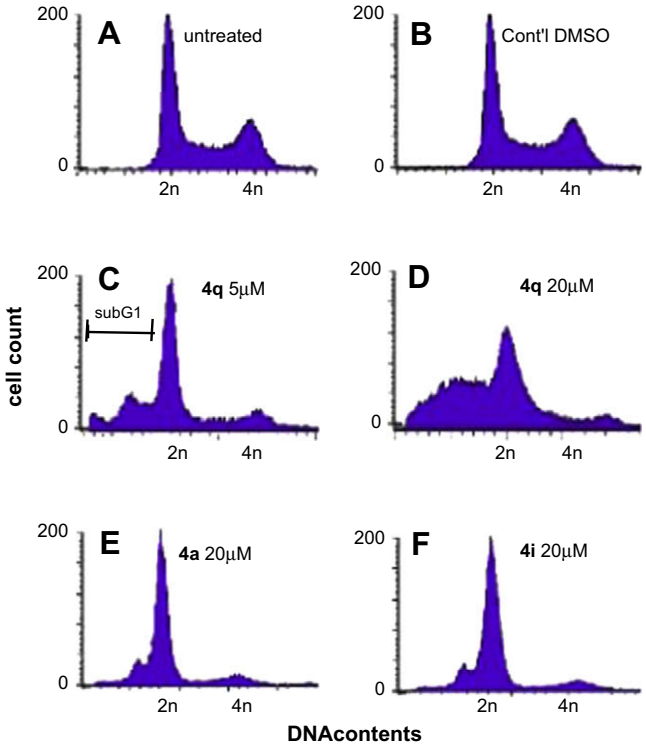

Fig. 4. Flow cytometric analysis of HeLa cells. Untreated HeLa cells were taken as blank group (A). Cells were treated with 0.5% DMSO as the control (B); compound **4q** 5 μM; (C) compound **4q** 20 μM; (D) compound **4a** 20 μM (E); or compound **4i** 20 μM (F). Cells were harvested after 24 h treatment and followed by fixation, propidium iodide staining as described in Section 4 prior to the flow cytometric analysis. Sub-G1 phase indicated the DNA fragmentation and cell death.

Restricted to the small size of our data set, the 17 compounds were all included in training set to build a CoMFA model. Model and the statistical results are listed in Fig. 6B. The optimal number of components (ONC = 5) was recommended after a leave-one-out cross-validated run with a q^2 of 0.459 which is acceptable for a small group of compounds. Generally a q^2 value close to or larger than 0.5 indicates the model is internally predictive and the future model built without cross-validation shall be accountable. The final training set model and coefficients such as R^2 and F-value were obtained by using the optimal number of components and all the data points in the training set. The obtained R^2 value of 0.860 is higher than the criteria value 0.6 for a fairly good model. To further ensure the predictive ability of the CoMFA model built by the training set, we carried out a series of test modeling (Pred-1, -2, -3, -4, and -5 columns in Fig. 6B) by deleting at random one data point from the training set to form new models and then predict the deleted compounds' pIC_{50} values. The test set predictions are given in bold in each Pred-column. Comparing the training and test set results, we found that the fractions of steric and electrostatic contributions to each model are similar and both contributions are nearly equally important.

Since **4a**–**4l** differ in substituents on ring-B, the lower-right fields derived from CoMFA model are applied for comparing their activities. Likewise, the left side fields surrounding ring-A are suitable to explain the inhibition performance of **4m**–**4q**. In Fig. 6A, the lower-right green region indicates a preference of bulky group that explains **4l** has a higher activity with an IC_{50} of 16.6 μM in

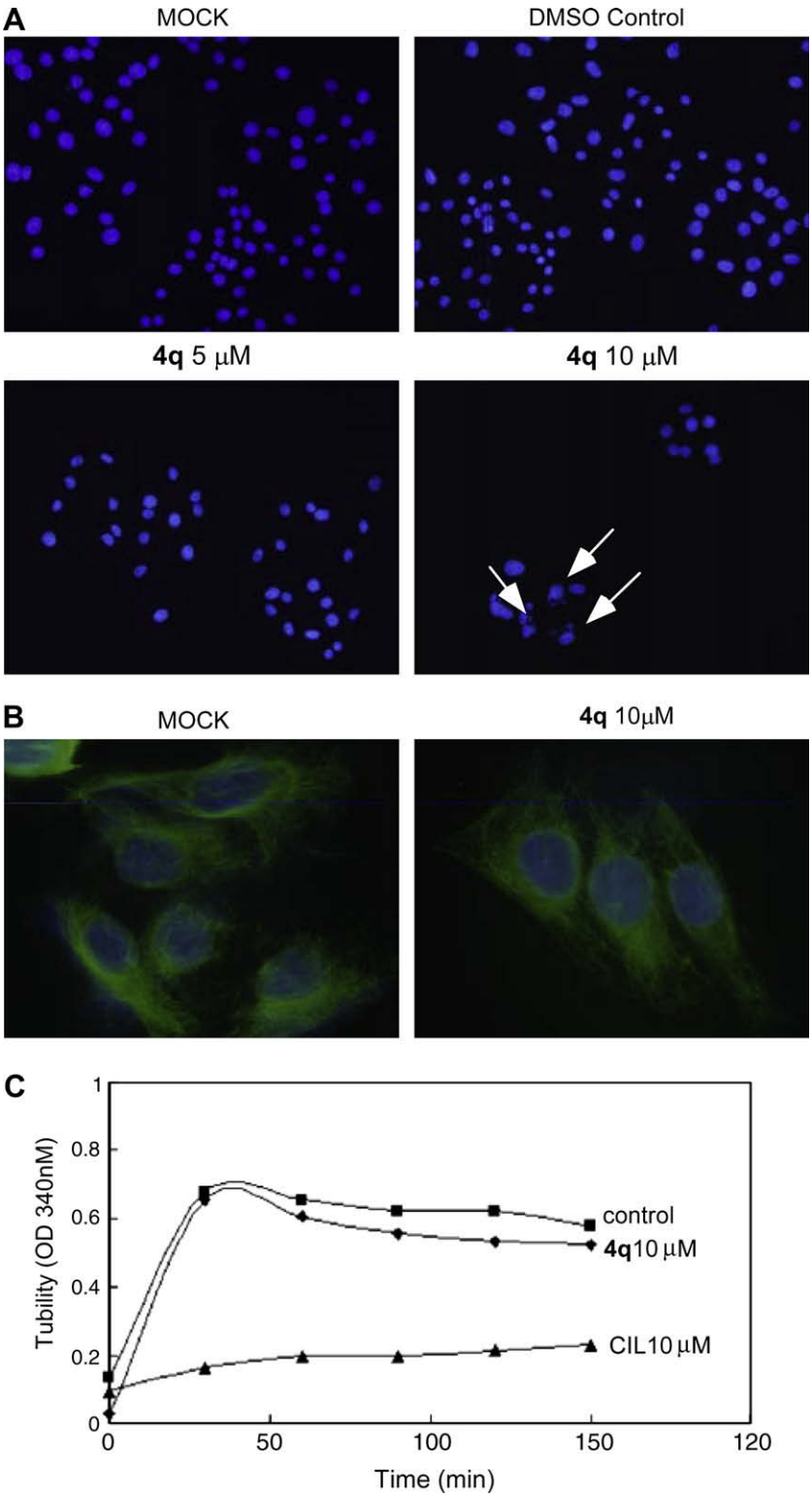

Fig. 5. DNA fragmentation and microtubule effect of compound **4q** on HeLa cells. (A) DAPI staining to examine the DNA fragmentation effect by compound **4q**. Untreated HeLa (Mock) or cells were treated with 0.5% DMSO as the control or treated with compound **4q** 5 μM or 10 μM. (B and C) Microtubule effect of compound **4q**. HeLa cells were fixed after 24 h **4q** treatment and followed by immunocytochemistry examination using anti-β-tubulin antibody, FITC-conjugated secondary antibody and DAPI staining as described in Section 4. Compound **4q** did not affect the tubulin polymerization in vitro by light scattering assay (C). CIL compound was used as positive control.

response to the longest side chain compared to other compounds. The lower-right red regions which prefer negatively charged groups or atoms explain why **4j** (IC_{50}, 26.6 μM) is better than **4i** ($IC_{50} > 40$ μM). That is, compared to the $-CF_3$ group in **4i**, the slightly longer $-OCF_3$ group in **4j** allows its negatively charged fluorine atoms to reach the red regions. As to the left side fields, the upper red region that prefers a negatively charged group is related to the R_5-substitution whereas the lower blue region that prefers

A

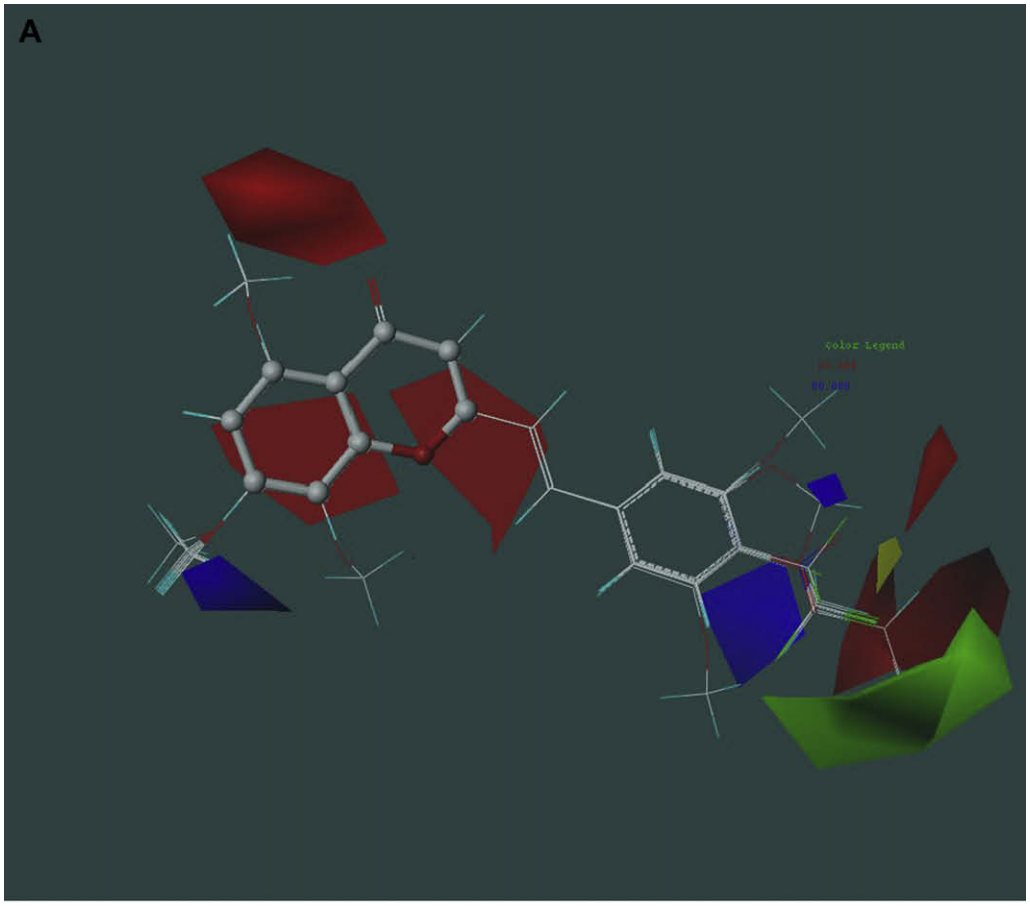

B

Compd	pIC_{50}	Training set	Pred-1	Pred-2	Pred-3	Pred-4	Pred-5
4b	4.60	4.611	4.611	4.610	4.628	**4.560**	4.618
4c	4.70	4.709	4.710	4.723	4.655	4.725	4.697
4d	4.58	4.448	4.447	4.442	4.444	4.421	4.447
4e	4.22	4.425	4.425	4.419	4.433	4.389	4.428
4f	4.53	4.496	4.494	**4.623**	4.527	4.543	4.520
4g	4.53	4.533	4.532	4.522	4.533	4.498	4.533
4h	4.78	4.765	4.766	4.762	4.779	4.782	4.764
4i	4.22	4.204	4.204	4.204	4.237	4.212	4.197
4j	4.58	4.584	**4.615**	4.571	4.584	4.597	4.595
4k	4.59	4.552	4.552	4.559	4.480	4.595	4.533
4l	4.78	4.791	4.790	4.779	**4.500**	4.769	4.817
4m	4.81	4.834	4.824	4.839	4.845	4.818	4.810
4n	4.74	4.725	4.734	4.712	4.766	4.724	4.718
4p	4.70	4.691	4.700	4.704	4.655	4.695	4.683
4q	4.51	4.502	4.502	4.493	4.522	4.502	**4.661**

parameter						0.420
q^2	0.459	0.362	0.429	0.493	0.337	0.420
ONC	5	5	5	3	6	4
STE	0.084	0.089	0.089	0.091	0.090	0.087
R^2	0.860	0.861	0.861	0.801	0.876	0.849
F value	11.013	9.893	9.905	13.385	8.248	12.617
Fraction						
Steric	0.554	0.553	0.535	0.569	0.485	0.607
Electrostatic	0.446	0.447	0.465	0.431	0.515	0.393

Fig. 6. A) Steric and electrostatic fields generated with the CoMFA model with training set data: yellow indicates regions where bulky groups decrease activity (contribution level of 80%) whereas green indicates regions where bulky groups increase activity (contribution level of 20%); red indicates regions where negatively charged groups increase activity (contribution level of 20%), whereas blue indicates regions where positively charged groups increase activity (contribution level of 80%). The core used in alignment protocol of Sybyl 8.0 program is specified in ball and stick. (B) Statistics of CoMFA analysis. (For interpretation of the references to color in this figure legend, the reader is referred to the web version of this article.)

a positively charged group is related to the R_3-substitution. These two regions can be used to interpret the different levels of activities of compounds **4n**, **4p**, and **4q** that have methoxy group on R_3 or R_5 site. Obviously, the negatively charged character of methoxy group in **4n**'s R_5 site fits in the red region and shows a better inhibition activity whereas the methoxy group in **4p** and **4q**'s R_3 sites violate the positive charge preference and show lower inhibition toward the BT483 cell line. Moreover, since the oxygen atom on methoxy group, by virtue of its high electronegativity, can inductively withdraw electron through σ-bonds. Consequently, among **4m**–**4q**, compound **4m** without any methoxy group exhibits the highest activity in accordance with the red regions around the two fused π rings that indicate a negative charge preference.

3. Conclusion

In conclusion, the present work described the synthesis of a series of 2-styrylchromone analogs as well as the evaluation of antiproliferative effects on five carcinoma cell lines. Only **4m** exhibited a moderate activity with an IC_{50} value of 28.9 μM against PC-3 cells which indicates the selective sensitivity of PC-3 cells in response to 2-styrylchromones. In addition, **4q** exhibited the most antiproliferative effect with an IC_{50} value of 4.9 μM against HeLa cells. Further flow cytometric analysis and DAPI staining revealed that **4q** showed its cytotoxic effects on HeLa cells through sub-G1 arrest and DNA fragmentation. Moreover, CoMFA analysis to study 3D-QSAR on BT483 cell line gave a q^2 value of 0.459. Taken together, these results suggest a potential structural optimization and more detailed pharmacological study of 2-styrylchromones.

4. Experimental

4.1. Chemistry

Chemical reagents and organic solvents were purchased from TCI and Alfa Aesar unless otherwise mentioned. Melting points were determined by Fargo MP-2D. Nuclear magnetic resonance spectra (^{1}H NMR) were measured on a Bruker AC-300 instrument. Chemical shifts (δ) are reported in parts per million relative to the TMS peak. Mass spectra were obtained by FAB on a Jeol JMS-700 instrument. Flash column chromatography was performed with silica gel (230–400 mesh). Elemental Analysis was carried out on a Heraeus VarioEL-III C, H, N analyzer.

4.1.1. General procedure

*4.1.1.1. 1-(2-Hydroxy-4,6-dimethoxy phenyl)ethanone (**2a**).* To a solution of 2′,4′,6′-trihydroxyacetophenone (**1a**, 5.0 g, 30.0 mmol), Me_2SO_4 (5.3 ml, 56 mmol), and anhydrous K_2CO_3 (8.2 g, 56 mmol) in acetone (90 ml) was stirred at room temperature for 18 h. The reaction mixture was filtered and evaporated *in vacuo*, followed by recrystallization from ether–hexane to afford **2a** (4.9 g, 83%) as a yellowish solid. M.p. 78–80 °C (lit [32] 78.5–79.5 °C). ^{1}H NMR (300 MHz, $CDCl_3$)^d 2.58 (s, 3H), 3.81 (s, 3H), 3.84 (s, 3H), 5.91 (d, J = 2.4 Hz, 1H), 6.05 (d, J = 2.3 Hz, 1H), 14.0 (s, 1H) ppm. ^{13}C NMR (75 MHz, $CDCl_3$)^d 32.9, 55.6, 90.7, 93.6, 106.1, 163.0, 163.2, 167.6, 203.3 ppm.

*4.1.1.2. 5,7-Dimethoxy-2-methyl-4*H*-chromen-4-one (**3a**).* A solution of **2a** (3.92 g, 20.0 mmol) in dry ethyl acetate (30 ml) was added sodium (2.76 g, 120 mmol), the reaction mixture was stirred at room temperature for 18 h. Cold 0.5 N HCl (30 ml) was added and the aqueous layer was separated, the remained organic layer was dried and evaporated *in vacuo* to obtain the crude diketone. A solution of the crude diketone with couple drops of concentrated HCl in methanol (50 ml) was stirred at room temperature for 4 h. The methanol was removed *in vacuo* to get the residue, followed by the addition of ethyl acetate (50 ml) and washed with brine (50 ml). The organic layer was dried, evaporated *in vacuo* and purified with silica gel chromatography to obtain **3a** (2.95 g, 67% in two steps). M.p. 120–121 °C. ^{1}H NMR (300 MHz, $CDCl_3$)^d 2.27 (s, 3H), 3.87 (s, 3H), 3.92 (s, 3H), 6.00 (s, 1H), 6.33 (d, J = 2.3 Hz, 1H), 6.41 (d, J = 2.3 Hz, 1H) ppm. ^{13}C NMR (75 MHz, $CDCl_3$) δ 19.7, 55.7, 56.3, 87.0, 92.6, 95.8, 108.7, 111.8, 135.5, 160.1, 160.8, 163.0, 163.7, 177.4, 207.9 ppm.

*4.1.1.3. (*E*)-5,7-Dimethoxy-2-styryl-4*H*-chromen-4-one (**4a**).* Sodium (0.69 g, 30.0 mmol) was gradually added to dry methanol (30 ml) and the mixture was stirred until the solution reached room temperature. **3a** (1.1 g, 5.0 mmol) and benzaldehyde (0.64 g, 6.0 mmol) were added and the resulting mixture was allowed to stir at reflux for 18 h. After this period, the solution was poured into iced water and the pH was adjusted to 4 with HCl. The yellow solid was removed by filtration, taken up in DCM and purified with silica gel chromatography (eluent DCM:ethyl acetate = 4:1) to give **4a** (1.1 g, 71%) as a white solid. M.p. 186–188 °C. ^{1}H NMR (300 MHz, $CDCl_3$) δ 3.88 (s, 3H), 3.90 (s, 3H), 6.13 (s, 1H), 6.31 (d, J = 2.3 Hz, 1H), 6.49 (d, J = 2.3 Hz, 1H), 6.55 (d, J = 16.2 Hz, 1H), 7.32 (m, 3H), 7.52 (d, J = 16.2 Hz, 1H), 7.69 (m, 2H) ppm. ^{13}C NMR (75 MHz, $CDCl_3$) δ 55.87, 56.48, 92.87, 96.10, 112.35, 120.03, 127.62, 129.68, 135.29, 135.62, 135.79, 159.18, 159.75, 160.99, 164.15, 177.71 ppm. HRMS $(M)^+$ calcd for $C_{19}H_{16}O_4$ 308.3279; found 308.1039. Anal. Calcd for $C_{19}H_{16}O_4$: C, 74.01; H, 5.23. Found: C, 73.89; H, 5.32.

*4.1.1.4. (*E*)-5,7-Dimethoxy-2-(2-pyridin-4-yl-vinyl)-chromen-4-one (**4b**).* Compound **4b** was synthesized from the procedure described for compound **4a**. M.p. 212–213 °C. 1H NMR (300 MHz, $CDCl_3$)^d 3.91 (s, 3H), 3.92 (s, 3H), 6.24 (s, 1H), 6.35 (d, J = 16.0 Hz, 1H), 6.37 (d, J = 2.3 Hz, 1H), 6.54 (d, J = 2.3 Hz, 1H), 6.85 (d, J = 16.0 Hz, 1H), 7.42 (m, 2H), 8.65 (m, 2H) ppm. ^{13}C NMR (75 MHz, $CDCl_3$)^d 55.9, 56.5, 92.9, 96.3, 113.9, 119.6, 124.3, 129.1, 132.4, 142.5, 150.7, 157.9, 159.7, 161.1, 164.4, 177.5 ppm. HRMS $(M)^+$ calcd for C18H15NO4 309.1001; found 309.0994. Anal. Calcd for C18H15NO4: C, 69.89; H, 4.89. Found: C, 69.76; H, 4.81.

*4.1.1.5. 2-[2-(4-Fluoro-phenyl)-vinyl]-5,7-dimethoxy-chromen-4-one (**4c**).* Compound **4c** was synthesized from the procedure described for compound **4a**. M.p. 169–171 °C. 1H NMR (300 MHz, CDCl3)^d 3.85 (s, 3H), 3.94 (s, 3H), 6.17 (s, 1H), 6.35 (d, J = 2.3 Hz, 1H), 6.53 (d, J = 2.3 Hz, 1H), 6.62 (d, J = 16.0 Hz, 1H), 7.10 (m, 2H), 7.43 (d, J = 16.0 Hz, 1H), 7.54 (m, 2H) ppm. ^{13}C NMR (75 MHz, $CDCl_3$)^d 55.9, 56.7, 92.9, 96.2, 109.6, 112.4, 116.1, 116.4, 119.9, 129.5, 131.6, 134.6, 159.1, 159.8, 161.9, 164.3, 177.8 ppm. HRMS $(M+1)^+$ calcd for C19H15FO4 326.0954; found 326.0952. Anal. Calcd for C19H15FO4: C, 69.93; H, 4.63. Found: C, 69.04; H, 4.58.

*4.1.1.6. 2-[2-(4-Chloro-phenyl)-vinyl]-5,7-dimethoxy-chromen-4-one (**4d**).* Compound **4d** was synthesized from the procedure described for compound **4a**. M.p. 171–172 °C. ^{1}H NMR (300 MHz, $CDCl_3$)^d 3.91 (s, 3H), 3.95 (s, 3H), 6.19 (s, 1H), 6.35 (d, J = 2.3 Hz, 1H), 6.54 (d, J = 2.3 Hz, 1H), 6.67 (d, J = 16.0 Hz, 1H), 7.37 (d, J = 8.5 Hz, 2H), 7.45 (d, J = 16.0 Hz, 1H), 7.49 (d, J = 8.5 Hz, 2H) ppm. ^{13}C NMR (75 MHz, $CDCl_3$)^d 55.9, 56.6, 92.9, 95.2, 112.7, 120.7, 127.1, 128.7, 129.4, 133.9, 134.4, 135.5, 158.9, 159.8, 161.1, 164.3, 177.6 ppm. HRMS $(M)^+$ calcd for C19H15ClO4 342.0659; found 342.0660. Anal. Calcd for C19H15ClO4: C, 66.58; H, 4.41. Found: C, 65.95; H, 4.52.

*4.1.1.7. 2-[2-(4-Bromo-phenyl)-vinyl]-5,7-dimethoxy-chromen-4-one (**4e**).* Compound **4e** was synthesized from the procedure described for compound **4a**. M.p. 172–173 °C. ^{1}H NMR (300 MHz, CDCl3)^d 3.91 (s, 3H), 3.94 (s, 3H), 6.19 (s, 1H), 6.35 (d, J = 2.3 Hz, 1H), 6.53 (d,

$J = 2.3$ Hz, 1H), 6.68 (d, $J = 16.0$ Hz, 1H), 7.42 (d, $J = 8.5$ Hz, 2H), 7.43 (d, $J = 16.0$ Hz, 1H), 7.54 (d, $J = 8.5$ Hz, 2H) ppm. ^{13}C NMR (75 MHz, $CDCl_3$)[d] 55.7, 56.4, 92.6, 95.9, 112.5, 120.5, 123.6, 128.8, 131.6, 134.1, 134.3, 158.7, 159.6, 160.9, 164.1, 174.3, 177.6 ppm. HRMS $(M+1)^+$ calcd for C19H16BrO4 388.2314; found 388.0143. Anal. Calcd for $C_{19}H_{15}BrO_4$: C, 58.93; H, 3.90. Found: C, 58.42; H, 3.92.

*4.1.1.8. 5,7-Dimethoxy-2-[2-(4-methoxy-phenyl)-vinyl]-chromen-4-one (**4f**).* Compound **4f** was synthesized from the procedure described for compound **4a**. M.p. 175–176 °C. ^{1}H NMR (300 MHz, $CDCl_3$)[d] 3.85 (s, 3H), 3.92 (s, 3H), 3.94 (s, 3H), 6.06 (s, 1H), 6.35 (d, $J = 2.3$ Hz, 1H), 6.54 (d, $J = 2.3$ Hz, 1H), 6.56 (d, $J = 16.0$ Hz, 1H), 6.91 (d, $J = 8.5$ Hz, 2H), 7.49 (d, $J = 16.0$ Hz, 1H), 7.51 (d, $J = 8.5$ Hz, 2H) ppm. ^{13}C NMR (75 MHz, $CDCl_3$)[d] 55.5, 55.8, 56.5, 92.8, 96.0, 109.5, 111.6, 114.5, 117.6, 119.6, 123.1, 128.1, 129.2, 135.5, 159.7, 160.9, 164.1, 177.8 ppm. HRMS $(M)^+$ calcd for $C_{20}H_{18}O_5$ 338.1154; found 338.1154. Anal. Calcd for $C_{20}H_{18}O_5$: C, 70.99; H, 5.36. Found: C, 70.23; H, 5.29.

*4.1.1.9. 2-(2-Benzo[1,3]dioxol-5-yl-vinyl)-5,7-dimethoxy-chromen-4-one (**4g**).* Compound **4g** was synthesized from the procedure described for compound **4a**. M.p. 217–218 °C. ^{1}H NMR (300 MHz, $CDCl_3$)[d] 3.87 (s, 3H), 3.89 (s, 3H), 6.00 (s, 2H), 6.12 (s, 1H), 6.33 (d, $J = 3.8$ Hz, 1H), 6.50 (d, $J = 15.9$ Hz, 1H), 6.51 (d, $J = 2.2$ Hz, 1H), 6.81 (d, $J = 7.9$ Hz, 1H), 6.99 (d, $J = 7.9$ Hz, 1H), 7.02 (d, $J = 3.8$ Hz, 1H), 7.38 (d, $J = 15.9$ Hz, 1H) ppm. ^{13}C NMR (75 MHz, $CDCl_3$)[d] 55.9, 56.6, 87.2, 92.9, 96.1, 101.7, 106.2, 108.8, 111.9, 119.5, 123.7, 129.9, 135.6, 148.6, 149.2, 159.5, 159.8, 161.1, 164.2, 177.8 ppm. HRMS $(M)^+$ calcd for C20H16O6 352.0947; found 352.0946. Anal. Calcd for C20H16O6: C, 68.18; H, 4.58. Found: C, 68.04; H, 4.44.

*4.1.1.10. 2-[2-(3,5-Dimethoxy-phenyl)-vinyl]-5,7-dimethoxy-chromen-4-one (**4h**).* Compound **4h** was synthesized from the procedure described for compound **4a**. M.p. 188–189 °C. ^{1}H NMR (300 MHz, CDCl3)[d] 3.83, 3.84 (s, 3H), (s, 3H), 3.92 (s, 3H), 3.94 (s, 3H), 6.17 (s, 1H), 6.35 (d, $J = 2.3$ Hz, 1H), 6.48 (d, $J = 2.3$ Hz, 1H), 6.54 (s, 1H), 6.65 (d, $J = 16.0$ Hz, 1H), 6.69 (s, 2H), 7.42 (d, $J = 16.0$ Hz, 1H) ppm. ^{13}C NMR (75 MHz, $CDCl_3$)[d] 55.6, 55.9, 55.6, 92.9, 96.2, 102.2, 105.7, 109.5, 112.5, 119.7, 120.6, 135.7, 137.2, 159.2, 159.8, 161.3, 164.3, 177.8 ppm. HRMS $(M)^+$ calcd for C21H20O6 368.1260; found 368.1263. Anal. Calcd for C21H20O6: C, 68.18; H, 4.58. Found: C, 68.04; H, 4.44.

*4.1.1.11. 5,7-Dimethoxy-2-[2-(4-trifluoromethyl-phenyl)-vinyl]-chromen-4-one (**4i**).* Compound **4i** was synthesized from the procedure described for compound **4a**. M.p. 201–202 °C. ^{1}H NMR (300 MHz, CDCl3)[d] 3.92 (s, 3H),3.95 (s, 3H), 6.22 (s, 1H), 6.37 (d, $J = 2.3$ Hz, 1H), 6.55 (d, $J = 2.3$ Hz, 1H), 6.78 (d, $J = 16.0$ Hz, 1H), 7.51 (d, $J = 16.0$ Hz, 1H), 7.65 (m, 4H) ppm. ^{13}C NMR (75 MHz, $CDCl_3$)[d] 55.9, 56.6, 75.4, 77.4, 92.7, 96.0, 109.4, 113.1, 119.3, 122.0, 122.4, 134.0, 138.5, 158.2, 159.5, 160.9, 164.1, 177.4 ppm. HRMS $(M)^+$ calcd for $C_{20}H_{15}F_3O_4$ 376.0922; found 376.0921. Anal. Calcd for $C_{20}H_{15}F_3O_4$: C, 63.83; H, 4.02. Found: C, 63.75; H, 4.13.

*4.1.1.12. 5,7-Dimethoxy-2-[2-(4-trifluoromethoxy-phenyl)-vinyl]-chromen-4-one (**4j**).* Compound **4j** was synthesized from the procedure described for compound **4a**. M.p. 155–156 °C. ^{1}H NMR (300 MHz, $CDCl_3$)[d] 3.92 (s, 3H), 3.94 (s, 3H), 6.19 (s, 1H), 6.35 (d, $J = 2.3$ Hz, 1H), 6.54 (d, $J = 2.3$ Hz, 1H), 6.66 (d, $J = 16.1$ Hz, 1H), 7.25 (d, $J = 6.9$ Hz, 2H), 7.53 (d, $J = 16.1$ Hz, 1H), 7.57 (d, $J = 6.9$ Hz, 2H) ppm. ^{13}C NMR (75 MHz, $CDCl_3$)[d] 55.7, 56.2, 75.4, 92.6, 95.9, 109.3, 112.5, 118.6, 121.1, 122.0, 125.4, 133.7, 149.7, 158.5, 159.5, 160.8, 164.0, 177.4 ppm. HRMS $(M)^+$ calcd for C20H15F3O5 392.0872; found 392.0876. Anal. Calcd for C20H15F3O5: C, 61.23; H, 3.85. Found: C, 61.07; H, 3.89.

*4.1.1.13. 5,7-Dimethoxy-2-[2-(4-nitro-phenyl)-vinyl]-chromen-4-one (**4k**).* Compound **4k** was synthesized from the procedure described for compound **4a**. M.p. 255–257 °C. ^{1}H NMR (300 MHz, $CDCl_3$)[d] 3.93 (s, 3H), 3.95 (s, 3H), 6.25 (s, 1H), 6.37 (d, $J = 2.3$ Hz, 1H), 6.55 (d, $J = 2.3$ Hz, 1H), 6.83 (d, $J = 16.0$ Hz, 1H), 7.52 (d, $J = 16.0$ Hz, 1H), 7.69 (d, $J = 8.6$ Hz, 2H), 8.26 (d, $J = 8.6$ Hz, 2H) ppm. ^{13}C NMR (75 MHz, $CDCl_3$)[d] 56.0, 56.7, 93.0, 96.4, 109.4, 114.1, 118.7, 124.5, 128.2, 133.0, 141.6, 148.2, 158.0, 159.8, 161.3, 164.6, 177.6 ppm. HRMS $(M)^+$ calcd for $C_{19}H_{15}NO_6$ 353.0899; found 353.0895.

*4.1.1.14. 2-[2-(4-Cyclopropylmethoxy-phenyl)-vinyl]-5,7-dimethoxy-chromen-4-one (**4l**).* Compound **4l** was synthesized from the procedure described for compound **4a**. M.p. 214–215 °C. ^{1}H NMR (300 MHz, $CDCl_3$)[d] 0.35 (m, 2H), 0.65 (m, 2H), 1.32 (m, 1H), 3.84 (d, $J = 6.9$ Hz, 2H), 3.91 (s, 3H), 3.94 (s, 3H), 6.14 (s, 1H), 6.34 (d, $J = 2.3$ Hz, 1H), 6.53 (d, $J = 2.3$ Hz, 1H), 6.54 (d, $J = 16.0$ Hz, 1H), 6.92 (d, $J = 8.8$ Hz, 2H), 7.43 (d, $J = 16.0$ Hz, 1H), 7.48 (d, $J = 8.8$ Hz, 2H) ppm. ^{13}C NMR (75 MHz, $CDCl_3$)[d] 3.16, 10.16, 55.7, 56.3, 72.8, 92.7, 95.8, 109.3, 111.4, 114.9, 117.4, 127.7, 128.9, 135.3, 159.5, 160.2, 160.8, 163.9, 177.6 ppm. HRMS $(M+16)^+$ calcd for $C_{23}H_{22}O_6$ 394.1416; found 394.1414. Anal. Calcd for $C_{23}H_{22}O_6$: C, 73.00; H, 5.86. Found: C, 71.45; H, 5.45.

*4.1.1.15. 2-Methyl-chromen-4-one (**3m**).* Compound **3m** was synthesized from the procedure described for compound **3a**. M.p. 55–56 °C. ^{1}H NMR (300 MHz, $CDCl_3$)[d] 2.37 (s, 3H), 6.16 (s, 1H), 7.33 (dd, $J = 7.7$, 1.6, 1H), 7.36 (dd, $J = 7.8$, 1.5 Hz, 1H), 7.62 (d, $J = 7.7$, 1H), 8.17 (dd, $J = 7.8$, 1.5 Hz, 1H) ppm. ^{13}C NMR (75 MHz, $CDCl_3$)[d] 20.5, 110.4, 117.7, 123.4, 124.8, 125.5, 133.4, 156.4, 166.2, 178.1 ppm.

*4.1.1.16. 2-[2-(4-Trifluoromethoxy-phenyl)-vinyl]-chromen-4-one (**4m**).* Compound **4m** was synthesized from the procedure described for compound **4a**. M.p. 169–171 °C. ^{1}H NMR (300 MHz, $CDCl_3$) 6.34 (s, 1H), 6.75 (d, $J = 16.1$ Hz, 1H), 7.25 (d, $J = 7.4$ Hz, 2H), 7.37 (m, 1H), 7.52 (d, $J = 7.4$ Hz, 2H), 7.55 (d, $J = 16.1$ Hz, 1H), 7.61 (m, 2H), 8.18 (d, $J = 7.9$ Hz, 1H) ppm. ^{13}C NMR (75 MHz, $CDCl_3$) 110.9, 115.2, 117.7, 118.6, 119.3, 122.0, 124.1, 125.0, 128.9, 133.6, 133.7, 135.0, 149.9, 155.9, 161.1, 178.3 ppm. HRMS $(M)^+$ calcd for C18H11F3O3 332.0660; found 332.0667. Anal. Calcd for C18H11F3O3: C, 65.06; H, 3.34C. Found: C, 64.48; H, 3.41.

*4.1.1.17. 1-(2-Hydroxy-6-methoxy-phenyl)-ethanone (**2n**).* Compound **2n** was synthesized from the procedure described for compound **2a**. M.p. 55–58 °C. ^{1}H NMR (300 MHz, $CDCl_3$)[d] 2.67 (s, 3H), 3.89 (s, 3H), 6.39 (d, $J = 4.5$ Hz, 1H), 6.56 (d, $J = 5.6$ Hz, 1H), 7.35 (m, 1H), 13.3 (s, 1H) ppm. ^{13}C NMR (75 MHz, $CDCl_3$)[d] 33.8, 56.8, 101.3, 110.8, 111.4, 135.7, 136.2, 161.7, 164.8, 205.3 ppm.

*4.1.1.18. 5-Methoxy-2-methyl-chromen-4-one (**3n**).* Compound **3n** was synthesized from the procedure described for compound **3a**. M.p. 97–98 °C. 1H NMR (300 MHz, $CDCl_3$)[d] 2.27 (s, 3H), 3.93 (s, 3H), 6.04 (s, 1H), 6.75 (d, $J = 8.2$ Hz, 1H), 6.94 (d, $J = 8.5$ Hz, 1H), 7.27 (dd, $J = 8.5$, 8.2 Hz, 1H) ppm. ^{13}C NMR (75 MHz, $CDCl_3$)[d] 19.9, 56.4, 106.3, 109.9, 112.1, 114.2, 133.5, 158.6, 159.7, 163.8, 178.3, 196.1 ppm.

*4.1.1.19. 5-Methoxy-2-[2-(4-trifluoromethoxy-phenyl)-vinyl]-chromen-4-one (**4n**).* Compound **4n** was synthesized from the procedure described for compound **4a**. M.p. 169–171 °C. ^{1}H NMR (300 MHz, $CDCl_3$)[d] 3.95 (s, 3H), 6.25 (s, 1H), 6.67 (d, $J = 16.1$ Hz, 1H), 6.81 (d, $J = 7.8$ Hz, 1H), 7.09 (d, $J = 8.0$ Hz, 1H), 7.24 (d, $J = 8.0$ Hz, 2H), 7.55 (d, $J = 16.1$ Hz, 1H), 7.61 (m, 3H) ppm. ^{13}C NMR (75 MHz, $CDCl_3$)[d] 56.5, 106.5, 109.9, 112.6, 114.7, 118.8, 119.5, 120.9, 121.3, 128.9, 133.8, 134.5, 149.9, 158.0, 159.1, 159.8, 178.3 ppm. HRMS $(M)^+$ calcd for C19H13F3O4 362.0766; found 362.0757. Anal. Calcd for $C_{19}H_{13}F_3O_4$: C, 62.99; H, 3.62. Found: C, 62.45; H, 3.74.

*4.1.1.20. 1-(2-Hydroxy-5-methoxy-phenyl)-ethanone (**2o**).* Compound **2o** was synthesized from the procedure described for compound **2a**. M.p. 48–50 °C. ^{1}H NMR (300 MHz, $CDCl_3$)^d 2.56 (s, 3H), 3.79 (s, 3H), 6.89 (d, J = 8.9 Hz, 1H), 7.09 (d, J = 8.9 Hz, 1H), 7.16 (s, 1H), 11.85 (s, 1H) ppm. ^{13}C NMR (75 MHz, $CDCl_3$)^d 11.7, 26.9, 56.1, 107.5, 113.6, 119.3, 124.3, 135.7, 151.8, 156.9, 194.8, 204.2 ppm.

*4.1.1.21. 6-Methoxy-2-methyl-chromen-4-one (**3o**).* Compound **3o** was synthesized from the procedure described for compound **3a**. M.p. 109–110 °C. ^{1}H NMR (300 MHz, $CDCl_3$)^d 2.37 (s, 3H), 3.74 (s, 3H), 6.15 (s, 1H), 7.22 (m, 1H), 7.33 (dd, J = 9.0, 2.8 Hz, 1H), 7.53 (d, J = 2.4 Hz, 1H) ppm. ^{13}C NMR (75 MHz, $CDCl_3$)^d 20.5, 55.8, 104.8, 109.7, 119.1, 123.2, 124.0, 151.2, 156.9, 165.9, 177.9 ppm.

*4.1.1.22. 6-Methoxy-2-[2-(4-trifluoromethoxy-phenyl)-vinyl]-chromen-4-one (**4o**).* Compound **4o** was synthesized from the procedure described for compound **4a**. M.p. 152–153 °C. ^{1}H NMR (300 MHz, $CDCl_3$)^d 3.89 (s, 3H), 6.26 (s, 1H), 6.75 (d, J = 16.0 Hz, 1H), 7.28 (m, 3H), 7.48 (d, J = 16.0 Hz, 1H), 7.59 (m, 4H) ppm. ^{13}C NMR (75 MHz, $CDCl_3$)^d 55.9, 105.0, 110.3, 118.8, 119.3, 121.3, 122.2, 123.7, 124.7, 129.0, 133.7, 134.8, 150.1, 150.8, 156.9, 161.0, 178.2 ppm. HRMS $(M)^+$ calcd for C19H13F3O4 362.0766; found 362.0768. Anal. Calcd for C19H13F3O4: C, 62.99; H, 3.62. Found: C, 61.38; H, 3.60.

*4.1.1.23. 1-(2-Hydroxy-4-methoxy-phenyl)-ethanone (**2p**).* Compound **2p** was synthesized from the procedure described for compound **2a** as a liquid. ^{1}H NMR (300 MHz, $CDCl_3$)^d 2.56 (s, 3H), 3.84 (s, 3H), 6.52 (s, 1H), 6.54 (d, J = 7.8 Hz, 1H), 7.63 (d, J = 7.8 Hz, 1H), 12.7 (s, 1H) ppm. ^{13}C NMR (75 MHz, $CDCl_3$)^d 26.3, 29.4, 55.7, 58.7, 100.9, 107.7, 114.0, 132.5, 165.4, 166.3, 202.8 ppm.

*4.1.1.24. 7-Methoxy-2-methyl-chromen-4-one (**3p**).* Compound **3p** was synthesized from the procedure described for compound **3a**. M.p. 106–108 °C. ^{1}H NMR (300 MHz, $CDCl_3$)^d 2.34 (s, 3H), 3.88 (s, 3H), 6.08 (s, 1H), 6.79 (d, J = 2.4 Hz, 1H), 6.92 (dd, J = 8.9, 2.4 Hz, 1H), 8.06 (d, J = 8.9 Hz, 1H) ppm. ^{13}C NMR (75 MHz, $CDCl_3$)^d 20.5, 55.8, 100.2, 110.4, 114.1, 117.4, 126.9, 158.2, 163.9, 165.7, 177.7 ppm.

*4.1.1.25. 7-Methoxy-2-[2-(4-trifluoromethoxy-phenyl)-vinyl]-chromen-4-one (**4p**).* Compound **4p** was synthesized from the procedure described for compound **4a**. M.p. 170–172 °C. ^{1}H NMR (300 MHz, $CDCl_3$)^d 3.94 (s, 3H), 6.23 (s, 1H), 6.74 (d, J = 16.0 Hz, 1H), 6.94 (m, 2H), 7.26 (m, 2H), 7.52 (d, J = 16.0 Hz, 1H), 7.62 (m, 2H), 8.08 (d, J = 8.9 Hz, 1H) ppm. ^{13}C NMR (75 MHz, $CDCl_3$)^d 55.9, 100.5, 111.2, 114.3, 118.1, 118.8, 121.4, 122.3, 127.2, 129.1, 133.9, 134.6, 150.1, 157.8, 160.9, 164.4, 177.9 ppm. HRMS $(M)^+$ calcd for $C_{19}H_{13}F_3O_4$ 362.0766; found 362.0771. Anal. Calcd for $C_{19}H_{13}F_3O_4$: C, 62.99; H, 3.62. Found: C, 62.54; H, 3.57.

*4.1.1.26. 1-(2-Hydroxy-3,4-dimethoxy-phenyl)-ethanone (**2q**).* Compound **2q** was synthesized from the procedure described for compound **2a**. M.p. 75–76 °C. ^{1}H NMR (300 MHz, $CDCl_3$)^d 2.56 (s, 3H), 3.87 (s, 1H), 3.92 (s, 3H), 6.47 (d, J = 9.0 Hz, 1H), 7.48 (d, J = 9.0 Hz, 1H), 12.55 (s, 1H) ppm. ^{13}C NMR (75 MHz, $CDCl_3$)^d 26.3, 56.1, 60.5, 102.9, 115.2, 127.1, 136.3, 156.9, 158.5, 203.3 ppm.

*4.1.1.27. 7,8-Dimethoxy-2-methyl-chromen-4-one (**3q**).* Compound **3q** was synthesized from the procedure described for compound **3a**. M.p. 86–88 °C. ^{1}H NMR (300 MHz, $CDCl_3$)^d 2.41 (s, 3H), 3.91 (s, 3H), 3.96 (s, 3H), 6.10 (s, 1H), 6.99 (d, J = 9.0 Hz, 1H), 7.90 (d, J = 9.0 Hz, 1H) ppm. ^{13}C NMR (75 MHz, $CDCl_3$)^d 20.7, 56.5, 61.6, 109.8, 110.1, 118.4, 121.0, 135.6, 136.6, 150.9, 156.4, 166.0, 178.0 ppm.

*4.1.1.28. 7,8-Dimethoxy-2-[2-(4-trifluoromethoxy-phenyl)-vinyl]-chromen-4-one (**4q**).* Compound **4q** was synthesized from the procedure described for compound **4a**. M.p. 181–182 °C. ^{1}H NMR (300 MHz, $CDCl_3$)^d 4.00 (s, 3H), 4.05 (s, 3H), 6.28 (s, 1H), 6.77 (d, J = 16.0 Hz, 1H), 7.03 (d, J = 9.0 Hz, 1H), 7.25 (d, J = 8.6 Hz, 2H), 7.59 (d, J = 16.0 Hz, 1H), 7.62 (d, J = 8.6 Hz, 2H), 7.93 (d, J = 9.0 Hz, 1H) ppm. ^{13}C NMR (75 MHz, $CDCl_3$)^d 56.6, 61.8, 109.9, 110.7, 118.8, 119.0, 121.3, 121.5, 128.2, 133.9, 135.2, 136.9, 150.2, 150.5, 157.0, 161.2, 178.2 ppm. HRMS $(M)^+$ calcd for C20H15F3O5 392.0872; found 392.0867. Anal. Calcd for $C_{20}H_{15}F_3O_5$: C, 61.23; H, 3.85. Found: C, 60.89; H, 3.78.

4.2. Antiproliferative activity

4.2.1. Cell culture

Cancer cells were purchased from Bioresource Collection and Research Center in Taiwan. Each cell line was maintained in the standard medium and grown as a monolayer in Dulbecco's Modified Eagle Medium (DMEM) containing 10% fetal bovine serum, 2 mM glutamine, 100 units/ml penicillin, and 100 g/ml streptomycin. Cultures were maintained at 37 °C with 5% CO_2 in a humidified atmosphere.

4.2.2. Antiproliferative assay

Cell proliferation and viability were measured by MTT assay. Compound stock solution (10 mM in DMSO) was prepared and stored at −20 °C, and was diluted with DMSO to 0.1–1 mM range at room temperature before experiment. The final percentage of DMSO in the reaction mixture was less than 1% (v/v). Cancer cells (1×10^4 cells/well) were plated in the 96-well plates and incubated in medium for 12 h. Serial dilutions of individual compounds were added. 3-[4,5-Dimethylthiazol-2-yl]-2,5-diphenyltetrazolium bromide, (2 mg/ml) (MTT, 20 ml) was added to the cultures and incubated during the final 1.5 h. The resultant tetrazolium salt was then dissolved by the addition of dimethylsulfoxide. Color was measured spectrophotometrically in a microtiter plate reader at 570 nm and used as a relative measure of viable cell number. The percentage of growth inhibition was calculated by using the equation: percentage growth inhibition = $(1-A_t/A_c) \times 100$, where A_t and A_c represent the absorbance in treated and control cultures, respectively. The compound concentration causing a 50% cell growth inhibition (IC_{50}) was determined by interpolation from dose–response curves.

4.2.3. Flow cytometric analysis

Apoptosis and cell cycle profile were assessed by DNA fluorescence flow cytometry. HeLa cells treated with DMSO or **4q** at a concentration of 10 μM for 24 h or 48 h were harvested, rinsed in PBS, resuspended and fixed in 80% ethanol, and stored at −20 °C in fixation buffer until ready for analysis. Then the pellets were suspended in 1 ml of fluorochromic solution (0.08 mg/ml PI (propidium iodide), 0.1% TritonX-100 and 0.2 mg/ml RNase A in 1 × PBS) at room temperature in the dark for 30 min. The DNA content was analyzed by FACScan flow cytometer (Becton Dickinson, Mountain View, CA) and CellQuest software (Becton Dickinson). The population of apoptotic nuclei (subdiploid DNA peak in the DNA fluorescence histogram) was expressed as the percentage in the entire population.

4.2.4. Immunofluorescence analysis

HeLa Cells were seeded on cover glasses in 12-well plates with the drug treatment for 24 h were used for DAPI staining. After incubation, cells were washed with 1 × PBS twice and fixed in 4% paraformaldehyde for 1 h. Then, cells were washed with PBS containing 0.1 M Glycine for 5 min and permibilized with solution containing 2% FBS and 0.4% TritonX-100 in PBS at room temperature for 15 min. After permibilization, cells were stained with α-tubulin monoclonal antibody (Santa Cruza 1:1000) at 4 °C overnight. After primary antibody incubation, cells were washed with

PBS containing 0.2% TritonX-100 three times, and stained with fluorescein isothiocyanate-conjugated anti-mouse IgG antibody (Santa Cruze, 1:200 diluted) at room temperature for 1 h. Finally, washed with PBS and stained with DAPI (0.1 μg/ml) for 5 min at room temperature in the dark. Removed the excess DAPI solution and washed with PBS twice. Mounted the samples before analyzing under a fluorescence microscopy.

4.2.5. In vitro microtubule polymerization assay

Tubulin proteins (>99% pure, minus glycerol, lyophilized) were purchased from Cytoskeleton Inc. The procedures were referred to the manufacture's indication. In brief, tubulin was suspended (300 μg/sample) with 100 μl of buffer (80 mM MOPS, 2 mM $MgCl_2$, 0.5 mM EGTA, 1 mM GTP) plus 5% glycerol in the absence or presence of test compound at 4 °C. Leave the protein on ice for 3 min then mix well with a pipette to make sure the protein has resuspended evenly. The sample mixture was transferred to the prewarmed eppendorf and incubated in 37 °C water bath for 2 min. The polymerization of tubulin was measured by the change in absorbance at 340 nm every 5 min for 60 min at 37 °C.

4.2.6. Statistical analysis

Data are presented as the mean ± sem (standard error of the mean) from four to six separated experiments. Statistical analyses were performed using Bonferroni *t*-test method after ANOVA for multigroup comparison and Student's *t*-test method for two-group comparison. $P = 0.05$ was considered significant. Analysis of linear regression (at least five data within 20–80% inhibition) was used to calculate IC_{50} value.

Acknowledgments

Financial support from the National Science Council of the Republic of China (NSC 96-2113-M-032-007-MY2) and Tamkang University to A.Y.S. is gratefully acknowledged. We are indebted to Professor Kuo-Wei Huang (NUS) for useful discussion.

References

[1] H.F. Schmid, Chem. Org. Naturst. 11 (1954) 124–179 Springer–Verlag, Vienna, Austria.
[2] D.K. Holdsworth, Planta Med. 22 (1) (1972) 54–58.
[3] G.P. Ellis, Chem. Heterocycl. Compd. 31 (1977) 455–480.
[4] S.S. Ghosal, B. Shripati, P. Mahendra, Y. Kumar, Phytochemistry 21 (12) (1982) 2943–2946.
[5] A.M. Edwards, J.B.L. Howell, Clin. Exp. Allergy 30 (6) (2000) 756–774.
[6] D.E. Pratt, M. Betty, J. Food Sci. 29 (1) (1964) 27–33.
[7] D. Donnelly, R. Geoghegan, C. O'Brien, E. Philbin, T.S. Wheeler, J. Med. Chem. 8 (6) (1965) 872–875.
[8] P.C. Djerngou, D. Gatsing, M. Tehuendem, B.T. Ngadjui, P. Tane, A.A. Ahmed, A.M. Gamal-Eldeen, G.I. Adoga, T. Hirata, T.J. Mabry, Nat. Prod. Commun. 1 (11) (2006) 961–968.
[9] W. Reanmongkol, S. Sanan, P. Panichayupakaranant, K.-M. Kim, J. Pharm. Biomed. Anal. 41 (8) (2003) 592–597.
[10] P.J. Houghton, Stud. Nat. Prod. Chem. 21 (2000) 123–155.
[11] A.M. Gamal-Eldeen, P.C. Djemgou, M. Tchuendem, B.T. Ngadjui, P. Tane, H. Toshifumi, Z. Naturforsch., C, Biosci. 62 (5/6) (2007) 331–338.
[12] W. Ren, Z. Qiao, H. Wang, L. Zhu, L. Zhang, Med. Res. Rev. 23 (4) (2003) 519–534.
[13] L.R. Kelland, Expert Opin. Investig. Drugs 9 (2000) 2903–2911.
[14] A.M. Senderowicz, E.A. Sausville, J. Natl. Cancer Inst. 92 (2000) 376–387.
[15] W.H. Gerwick, J. Nat. Prod. 52 (2) (1989) 252–256.
[16] W.H. Gerwick, A. Lopez, G.D. Van Duyne, J. Clardy, W. Ortiz, A. Baez, Tetrahedron Lett. 27 (18) (1986) 1979–1982.
[17] G. Doria, C. Romeo, A. Forgione, P. Sberze, N. Tibolla, M.L. Corno, G. Cruzzola, G. Cadelli, Eur. J. Med. Chem. 14 (1979) 347–351.
[18] N. Desideri, C. Conti, P. Mastromarino, F. Mastropaolo, Antivir. Chem. Chemother. 11 (2000) 373–381.
[19] D. Brion, G. Le Baut, F. Zammatio, A. Pierre, G. Atassi, L. Belachm, Chem. Abstr. 116 (1991) 106092k.
[20] J. Marinho, M. Pedro, D.C.G.A. Pinto, A.M.S. Silva, J.A.S. Cavaleiro, C.E. Sunkel, M.S.J. Nascimento, Biochem. Pharmacol. 75 (4) (2008) 826–835.
[21] K. Momoi, Y. Soshiaki, M. Ishihara, K. Satoh, H. Kikuchi, K. Hashimoto, I. Yokoe, H. Nishikawa, S. Fujisawa, H. Sakagami, In Vivo 19 (1) (2005) 157–163.
[22] P. Filipe, A.M.S. Silva, P. Morliere, C.M. Brito, L.K. Patterson, G.L. Hug, J.N. Silva, J.A.S. Cavaleiro, J.- C. Maziere, J.P. Freitas, R. Santus, Biochem. Pharmacol. 67 (12) (2004) 2207–2218.
[23] A. Gomes, E. Fernandes, A.M.S. Silva, C.M.M. Santos, D.C.G.A. Pinto, J.A.S. Cavaleiro, J.L.F.C. Lima, Bioorg. Med. Chem. 15 (18) (2007) 6027–6036.
[24] Y. Karton, J.- L. Jiang, X.- D. Ji, N. Melman, M.E. Olah, G.L. Stiles, K.A. Jacobson, J. Med. Chem. 39 (1996) 2293–2301.
[25] E. Fernandes, F. Carvalho, A.M.S. Silva, C.M.M. Santos, D.C.G.A. Pinto, J.A.S. Cavaleiro, M.L. Bastos, J. Enzyme Inhib. Med. Chem. 17 (2002) 45–48.
[26] U.S. Cheema, K.C. Gulati, K. Venkataraman, J. Chem. Soc. (1932) 925.
[27] W.A. Price, A.M.S. Silva, J.A.S. Cavaleiro, Heterocycles 36 (11) (1993) 2601–2611.
[28] C.A. Gray, P.T. Kaye, A.T. Nchinda, J. Nat. Prod. 66 (8) (2003) 1144–1146.
[29] T.A. Geissman, J. Am. Chem. Soc. 73 (1951) 3514–3515.
[30] N.R. Ayyangar, R.A. Khan, V.H. Deshpande, Tetrahedron Lett. 29 (19) (1988) 2347–2348.
[31] T. Mosman, J. Immunol. Methods 65 (1–2) (1983) 55–63.
[32] K. Ichino, H. Tanaka, K. Ito, T. Tanaka, M. Mizuno, J. Nat. Prod. 51 (5) (1988) 906–914.